

6-18-2010

Interaction of extracellular domain 2 of the human retina-specific ATP-binding cassette transporter (ABCA4) with all-trans-retinal.

Esther E Biswas-Fiss
Thomas Jefferson University

Deepa S Kurpad
Thomas Jefferson University

Kinjalben Joshi
Thomas Jefferson University

Subhasis B Biswas
University of Medicine and Dentistry of New Jersey

Follow this and additional works at: https://jdc.jefferson.edu/bioscience_technologiesfp

 Part of the [Chemistry Commons](#)

[Let us know how access to this document benefits you](#)

Recommended Citation

Biswas-Fiss, Esther E; Kurpad, Deepa S; Joshi, Kinjalben; and Biswas, Subhasis B, "Interaction of extracellular domain 2 of the human retina-specific ATP-binding cassette transporter (ABCA4) with all-trans-retinal." (2010). *Department of Medical Laboratory Sciences & Biotechnology Faculty Papers*. Paper 1.

https://jdc.jefferson.edu/bioscience_technologiesfp/1

This Article is brought to you for free and open access by the Jefferson Digital Commons. The Jefferson Digital Commons is a service of Thomas Jefferson University's [Center for Teaching and Learning \(CTL\)](#). The Commons is a showcase for Jefferson books and journals, peer-reviewed scholarly publications, unique historical collections from the University archives, and teaching tools. The Jefferson Digital Commons allows researchers and interested readers anywhere in the world to learn about and keep up to date with Jefferson scholarship. This article has been accepted for inclusion in Department of Medical Laboratory Sciences & Biotechnology Faculty Papers by an authorized administrator of the Jefferson Digital Commons. For more information, please contact: JeffersonDigitalCommons@jefferson.edu.

As submitted to:

Journal of Biological Chemistry

And later published as:

“Interaction of Extracellular Domain 2 of the Human Retina-specific ATP-binding Cassette Transporter (ABCA4) with All-*trans*-retinal”

Volume 285, Issue 25, 18 June 2010, Pages 19372-19383

DOI: 10.1074/jbc.M110.112896

Esther E. Biswas-Fiss^{*1,2}, Deepa S. Kurpad¹, Kinjalben Joshi^{1, and} Subhasis B. Biswas

[‡]Department of Bioscience Technologies, Program in Biotechnology, JSHP, Thomas Jefferson University, Philadelphia, PA 19107 and Department of Molecular Biology; University of Medicine and Dentistry of New Jersey, SOM, Stratford, NJ 08084.

Running Head: Second Extracellular Domain of ABCA4.

*Address correspondence to: Esther E. Biswas-Fiss, Department of Bioscience Technologies, Thomas Jefferson University, Edison Bldg. Suite 1924, 130 South 9th Street, Philadelphia, PA 19107 Tel. 215 503-8184; Fax. (215) 503-2189; E-mail: Esther.Biswas@jefferson.edu

The retina-specific ABC transporter, ABCA4, is essential for transport of all-*trans* retinal from the rod outer segment discs in the retina and is known to be associated with a broad range of inherited retinal diseases including, Stargardt disease (STGD), autosomal recessive cone rod dystrophy (arCRD) and fundus flavimaculatus (FFM). A unique feature of the ABCA subfamily of ABC transporters is the presence of highly conserved, long extracellular loops or domains (ECDs) with unknown function. The high degree of sequence conservation and mapped disease associated mutations in these domains suggest an important physiological significance. Conformational analysis using circular dichroic spectroscopy of purified, recombinant ECD2 protein demonstrated that it has an ordered and stable structure comprised of 27±3% α -helix, 20±3% β -pleated sheet, and 53±3% coil.

Significant conformational changes were observed in disease-associated mutant proteins. Using intrinsic tryptophan fluorescence emission spectrum of ECD2 polypeptide, we have demonstrated that this domain specifically interacts with all-*trans* retinal with a K_d of 1.3×10^{-7} M. Furthermore, the retinal interaction appeared specific for the all-*trans* isomer, and was directly measurable through fluorescence anisotropy analysis of all-*trans* retinal. This interaction was impaired in mutant ECD2 proteins. In summary, our results demonstrate that the three macular degeneration-associated mutations lead to significant changes in the secondary structure of the ECD2 domain of ABCA4, as well as in its interaction with all-*trans*-retinal.

ABC transporters are required for transport of a wide variety of hydrophobic

substances across cellular membranes, including drugs (1-3), lipids (4-6), metabolites, peptides (7), and steroids (2). Typically, eukaryotic ABC proteins are comprised of two tandem sets of six transmembrane helices followed by a Walker type A and a type B nucleotide-binding motif (8). To date, 48 members of the human ABC transporter family have been identified, which, based on sequence homology, have been divided into seven subfamilies, ABCA through ABCG (2-3,9).

A retina specific variant of the ABCA subfamily, the ABCA4 gene product (ABCR) was first described as the bovine and *Xenopus* Rim proteins identified in the rims of the rod outer segment (ROS) discs (10-11). Mutations in the ABCA4 gene appear to lead to defects in the energy-dependent transport of all-*trans* retinal and lead to the accumulation of cytotoxic lipofuscin fluorophores in the retinal pigment epithelium characteristic of the diseases such as Stargardt disease (STGD), fundus flavimaculatus (FFM) and autosomal recessive cone-rod-dystrophy (arCRD), as well as increased susceptibility to age-related macular degeneration (AMD) (12-20). Although ultimately these diseases await the promise of a cure through gene therapy (21-22), current treatments have been directed towards slowing the progression of the disease. Consequently, understanding how genetic mutations lead to retinal degeneration is critical for the development of experimental therapies.

Studies in several laboratories and the establishment of ABCA4 screening consortiums have aided in the identification of over 500 mutations in ABCA4 gene that are associated with a plethora of visual diseases. A genotyping microarray chip has been developed for the ABCA4 gene which can robustly identify >98% of the existing mutations (23). Disease-associated ABCA4 alleles have shown an extraordinary genetic heterogeneity. Some of these mutations map to the nucleotide binding domains (NBDs), suggesting that the underlying defect has a basis in nucleotide hydrolysis and/or aspects of energy transduction related to transport. However, the fact that ABCA4 mutations occur throughout the entire open reading frame, suggest that defects in ATP hydrolysis only are one of the causes of these diseases. At present, the biochemical basis of functional defects due to mutations in domains other than the NBDs remain refractory to

biochemical analysis, primarily because these domains lack any known enzymatic function.

Structural topology varies significantly between the eight subclasses of ABC transporters. In the ABCA subfamily each half transporter contains a transmembrane domain (TMD) comprised of six membrane spanning units, followed by a cytoplasmic or soluble domain. In addition, each ABCA half transporter possesses a large extracellular loop, which is characteristic of this subfamily. In the case of ABCA4, several models of membrane topology have been proposed based on hydropathy profiles, and experimental data supports the notion that two large extracellular domains (ECDs) are present (24). The EC loops project from TMD1 for ECD1 and from TMD7 for ECD2; they represent significantly large polypeptide domains, with 603 residues for ECD1 (aa 43–646) and 285 residues for ECD2 (aa 1395–1680). The high degree of sequence conservation observed in the ECDs of vertebrate ABCA4 proteins suggests an important physiological significance (20,25).

In the absence of any known enzymatic or functional motif, it has been difficult to assess the significance of disease-associated mutations in the ECD domains of ABCA4. Expression and characterization of individual functional domains has been demonstrated to be a viable approach utilized by several laboratories working with other ABC proteins, such as the MDR1 and CFTR transporters (26-29). ABCA4 is a particularly large membrane protein (~220 kDa), which is fairly unstable as a recombinant whole molecule. Consequently, systematic analysis of the structure and function of each individual domain in recombinant form is a highly viable and specific approach, as demonstrated by our previous studies with the NBD1/NBD2 domains of ABCA4. Previously, we were able to delineate the structural and functional specificities of the individual nucleotide binding domains which would not have been possible using the full-length ABCA4 protein (30-32).

Fluorescence and CD spectroscopic methodologies have been utilized as valuable tools for the characterization of structure and function of a variety of proteins including ABC transporters (33-35). In this report we have employed these techniques to elucidate the structural features and functional properties of the second extracellular

loop of ABCA4 as well as to delineate the effects of disease-associated mutations in the ECD2 domain.

EXPERIMENTAL PROCEDURES

Nucleic Acids, Enzymes, and Other Reagents. The pRK5 plasmid containing the full-length, wild-type cDNA of the human ABCA4 gene was obtained as a generous gift from Drs. J. Nathans and Michael Dean of Johns Hopkins University (Baltimore, MD) and NCBI (Frederick, MD) respectively. The T7 expression system vector pET30b, Bug Buster protein extraction reagent, Benzonase nuclease and the S-protein agarose affinity resin were from Novagen (EMD Sciences; Briggstown, NJ). All-*trans* retinal was from Sigma/Aldrich (St. Louis, MO) while 11-*cis* retinal was synthesized by Toronto Research Chemicals, Canada.

Buffers -- Buffer A was 20 mM Tris-HCl (pH 8.0), 100 mM NaCl, 2 mM dithiothreitol, and 15% (v/v) glycerol. Buffer B contained 20 mM Tris-HCl (pH 7.5), 1 mM MgCl₂, 50 mM NaCl, 5% glycerol, and 0.01% Nonidet P-40. Buffer C was 6 M guanidine hydrochloride, 0.1 M Tris-HCl (pH 8.0), and 2 mM EDTA. Buffer D contained 0.1 M Tris-HCl (pH 8.0), 0.5 M L-arginine, and 2 mM EDTA. Buffer E contained 10 mM NaPO₄ (pH 7.4), 100 mM NaCl, and 2 mM dithiothreitol.

Design and Cloning of the Construct Containing ECD2. The ECD2 construct was amplified from full-length ABCA4 cDNA and cloned into pET30b T7-expression vector (EMD Sciences; Briggstown, NJ) using standard recombinant DNA technology (36). This domain corresponds to a 31.8 kDa (285 aa) polypeptide. The cloning was designed such that the polypeptide was produced as a S-tagged fusion protein, leading to a predicted mass of 34.4 kDa for the recombinant ECD2. For subsequent recombinant protein expression, the plasmid was used to transform *E. coli* strain BL21-CodonPlus(DE3)-RILP competent cells (Stratagene, La Jolla, CA).

In Vitro Site-directed Mutagenesis of the ECD2 Construct. Site-directed mutagenesis was carried out using a PCR based mutagenesis kit (Stratagene, La Jolla, CA) (32) and the pET30-ECD2 plasmid as template. The complementary oligonucleotides used as mutagenic primers to generate the mutant ECD2 proteins as detailed in

Table 1. The authenticity of the mutations and the absence of other fortuitous mutations were confirmed by DNA sequencing carried out by Eurofins MWG/Operon (Huntsville, AL).

Over Expression of pET30b-ECD2 in E. coli. *E. coli* cells (strain BL21-CodonPlus(DE3)-RILP; Stratagene; LaJolla, CA) harboring pET30b-ECD2 plasmid were used to produce the recombinant ECD2 polypeptide following the manufacturer's instructions. The expressed recombinant polypeptide appeared to be of the anticipated size (34 kDa), as determined by SDS-PAGE (Fig. 3A).

Extraction and Purification of Recombinant ECD2 Proteins—Extraction and purification of wild-type ECD2 protein carrying the S-tag using immobilized S-protein agarose affinity resin (EMD Chemicals; Gibbstown, NJ) following the manufacturer's recommendations as previously described (30).

Purification of ECD2 Polypeptide from Solubilized Inclusion Bodies. Introduction of mutations into wild-type ECD2 polypeptide appeared to decrease the solubility of the expressed proteins as determined by SDS-PAGE and Western blot procedure (data not shown). Consequently, we explored the extraction of recombinant proteins (wild-type and mutants) from the inclusion bodies followed by refolding. (37) This approach has been shown to be highly successful in the purification of a number of ABC transporters (32,38-40).

The wild-type and mutant ECD2 proteins were extracted from inclusion bodies using a protocol, which combines the use of BugBuster protein extraction reagent (Novagen, Madison, WI) to process the insoluble fraction and yield purified inclusion bodies, with the method described by Booth et al. (32,38,41). After harvesting the expressed proteins, the cell pellets were resuspended in room temperature BugBuster reagent, and protease inhibitors were added. After incubation on ice for 30 minutes, the cell suspension was centrifuged to collect purified inclusion bodies. Following cell lysis, the pellet of inclusion bodies was resuspended in buffer B and centrifuged once more. The inclusion body proteins were solubilized in Buffer C. Protein refolding was achieved by rapid dilution in Buffer D. The renatured protein was sequentially dialyzed in Buffer E. After overnight dialysis, proteins were concentrated to ~0.5 mg/ml by ultrafiltration

(Amicon/Millipore). Overall the inclusion body protein purification methodology described here yielded highly concentrated, purified, and homogeneous preparations of protein. The yield of ECD2 protein was >10 mg from 4 liters of induced cell culture. Purified proteins were stored at -80 °C until use.

Circular Dichroism Spectropolarimetry. Spectra were collected on a Jasco-810 spectropolarimeter (X-Ray and Structure Core Facility of ThomasJefferson University) using a 5 mm path length cell, and the temperature was maintained at 25°C, or indicated temperature, using a Peltier controlled cell holder. Spectra were the average of five scans collected at a speed of 10 nm min⁻¹. CD spectra were analyzed using the K2D2 neural network based method (<http://www.ogic.ca/projects/k2d2/>), with its associated web server to estimate protein secondary structure (42-43).

For thermal melting experiments, the ellipticity at 220 nm was monitored over a temperature range of 20-80°C, using a resolution of 0.2°C, a bandwidth of 1 nm, and a temperature gradient of 1°C min⁻¹. Global analysis of the data was conducted using the PRISM program (GraphPad Software, Inc.).

Steady-State Fluorescence Measurements- Fluorescence experiments were performed using a Fluorolog-2 spectrofluorometer (Jobin Yvon Horiba Inc., Edison, NJ), and measurements were made in an L-format configuration of excitation and emission channels. The excitation wavelength was set to 295 nm to avoid excitation of either tyrosine or phenylalanine residues. Emission was scanned from 320 to 400 nm. Excitation and emission slits were set at 8 nm and 4 nm respectively. The spectra of the ECD2 polypeptide were measured in a 0.1 mg/ml solution in buffer E. Changes in steady state fluorescence were used to monitor interaction with all-trans and 11-cis retinal over a concentration range of 0-15 µM. Titrations with increasing amounts of all-trans retinal were conducted and emission scans from 320 to 400 nm were taken at each concentration. Fluorescence data were normalized to 0-100 arbitrary units for wild type ECD2 and each mutant. A semilog plot of emission at 333 nm versus log [all-trans retinal] was fitted to the sigmoidal dose-response equation:

$$y = y_{\min} + (y_{\max} - y_{\min})/[1 + 10^{(\log K_d - X)}]$$

where y is the fluorescence intensity and x is the log of the all-trans retinal concentration.

Anisotropy values were expressed as millianisotropy, or mA (anisotropy divided by 1000). The standard error for the measured anisotropy values was ± 3 mA. An anisotropy reading for each titration point was taken three times for 10 s and averaged. The total fluorescence intensity did not change significantly with an increase in the ECD2 concentration. Therefore, fluorescence lifetime changes, or the scattered excitation light, did not affect the anisotropy measurements. Anisotropy, A, is defined as

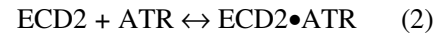
$$A = (I_{vv} - GI_{vh})/(I_{vv} + 2GI_{vh}) \quad (1)$$

where G is the instrumental correction factor for the fluorometer, and it is defined by,

$$G = I_{hv}/I_{hh}$$

where, I_{vv} , I_{vh} , I_{hv} , and I_{hh} represent the fluorescence signal for excitation and emission with the polarizers set at (0°, 0°), (0°, 90°), (90°, 0°), and (90°, 90°), respectively.

The interaction of ECD2 with all-trans retinal (ATR) can be represented as



At equilibrium, K_a , the equilibrium association constant, can be given as

$$K_a = [\text{ECD2}\bullet\text{ATR}]/[\text{ECD2}][\text{ATR}] \quad (3)$$

$$K_a = [\text{ECD2}][\text{ATR}] = [\text{ECD2}\bullet\text{ATR}] \quad (4)$$

The fraction of the binding sites occupied can be represented as

$$f = [\text{occupied binding sites}]/[\text{total binding sites}] =$$

$$[\text{ECD2}\bullet\text{ATR}]/([\text{ECD2}] + [\text{ECD2}\bullet\text{ATR}]) \quad (5)$$

Substituting for [ECD2] and rearranging the equation, we get

$$f = K_a(\text{ECD2})/[1 + K_a(\text{ECD2})] \quad (6)$$

$$f = [\text{ECD2}]/([\text{ECD2}] + 1/K_a) \quad (7)$$

Similarly, the equilibrium dissociation constant K_d ($(K_d)/K_a$) can be expressed as

$$f = [\text{ECD2}]/([\text{ECD2}] + K_d)$$

At $f = 0.5$

$$K_d = [\text{ECD2}]$$

Thus, K_d can be further defined as the protein concentration at which half of the sites are occupied when the ligand concentration is constant as in the present case or the ligand concentration at which half of the sites are occupied when the protein concentration is constant. Global analysis of the data was conducted using BIOEQS and/or PRISM (Graphpad Software Inc., San Diego, CA) programs using a monomer ligand binding model (44-45). BIOEQS calculates the concentration of various species in the equilibrium-binding curve numerically using a constrained optimization algorithm in which the mass balance constraints are incorporated as Lagrange multipliers (37). The program then relates this species concentration vector to the anisotropy observed at each point in the titration and fits the free energy and plateau values by adjusting these floating parameters using a Marquardt-Levenberg nonlinear least squares algorithm (46). The K_d values, i.e., the concentrations of ECD2 required to bind 50% of the all-*trans* retinal, were computed using the equation:

$$Y = A_{\min} + (A_{\max} - A_{\min}) / (1 + 10^{(X-X_0)/n_{\text{app}}}) \quad (10)$$

where A_{\min} and A_{\max} are the anisotropy values at the bottom and top plateaus, respectively, X represents the log of the NBD1 concentration, X_0 is the X value when the response is halfway between the top and the bottom, and n_{app} is the Hill coefficient.

Other Methods. Routine protein concentrations were determined by the method of Bradford (47) using bovine serum albumin as a standard, and for the CD/fluorescence studies using molar extension coefficient measurements $\epsilon_{\text{ECD2}} = 49,180$. SDS-PAGE was carried out as described by Lamelli (48).

RESULTS

The long extracellular (EC) loops, or domains, are a distinctive topological feature of the ABCA subfamily of transporters, yet at the present time their structure and function remain unknown. Based on current models (Fig. 1), the ECD1 domain of ABCA4 is defined as projecting from TMD1 (aa 43-646) while ECD2 projects from TMD7 (aa 1395-1680). We have calculated the grand average of hydropathicity indexes (GRAVY) for ECD1 and ECD2. GRAVY analysis of the domains were found to be -0.294 and -0.356 for ECD1 and ECD2, respectively (ProtParam; ExPASy Proteomics Server). A negative value corresponds to a hydrophilic polypeptide while a positive value corresponds to hydrophobic polypeptide, thus the values are consistent with the postulated projection of these domains into the aqueous environment of the lumen of the rod outer segment discs (Fig. 1) (49). *Stargardt Disease Mutations Affecting Conserved Residues of ECD2.* Several macular degenerative disease associated mutations map to the ECD2 domain of ABCA4 (13,23,50-52), pointing to its likely significance ABCA4 function. Three ABCA4 mutations associated with Stargardt disease, W1408L, R1443H, and C1488R, were chosen for analysis in this study. These missense mutations have been observed to occur in patients as simple and/or compound heterozygotes (Table 1). Sequence alignments of the ECD2 domains of ABCA4 proteins were carried out in order to determine the degree of conservation of these specific amino acid residues among the ECDs of several organisms. All three of the mutations correspond to strictly conserved amino acids in vertebrate ABCA4 proteins (Fig. 2).

Conformational Analysis of Native and Refolded ECD2 Polypeptides Suggest a Highly Ordered Structure: The structural characteristics of native and refolded recombinant ECD2 polypeptides were evaluated by comparing their CD spectra in the far ultra-violet region (200-250 nm). Highly purified homogenous preparations of recombinant ECD2 protein was used for CD analysis (Fig. 3). Secondary structures were determined using K2D2 neural network based analysis (<http://www.ogic.ca/projects/k2d2/>) (42).

The CD spectra of the native and refolded ECD2 polypeptides are presented in Fig. 4. The two spectra were essentially identical and were typical of structurally ordered proteins, containing

α -helical, β -sheet, and extended coil structures. Both CD spectra had two minima observed at 208 and 222 nm, characteristic of α -helical structure (Fig. 4). Nonlinear regression analysis of the CD spectra provided an estimation of ECD2 secondary structure; $26\pm 3\%$ α -helix and $23\pm 3\%$ β -sheet, respectively (Table 2). These results suggest that the structure of the refolded ECD2 polypeptide is essentially the same as that of the native ECD2 protein. We have analyzed changes in the conformation of ECD2 protein harboring disease associated mutations, W1408L, C1488R, and R1443H. The secondary structures of these proteins were then compared with that of the wild type polypeptide (Figs. 5 & 6).

W1408L Mutation – The W1408L mutation has been reported in several studies investigating the ABCA4 genotype of individuals afflicted with Stargardt disease, fundus flavimaculatus and cone rod dystrophy (13,19,51). This mutation has been identified in patients with and without the occurrence of a second ABCA4 mutation occurring in trans. Alone, this mutation leads to late onset (30 years of age) of Stargardt disease, whereas, patients harboring a second ABCA4 mutation in trans may manifest as early onset (12 years of age) of the disease. The Trp \rightarrow Leu mutation represents a relatively significant mutation, in terms of structure and polarity. In addition, the aromatic residue, with its large hydrophobic surface present in tryptophan, represents a potential “hotspot” for protein-protein and protein-ligand interactions and thus may alter the biological function of this domain (53). The far-UV CD spectrum of the mutant ECD2 was similar to that of the wild type protein suggesting that this mutant maintained most of the secondary structural features associated with wild type ECD2, (Fig. 5). Nonlinear regression analysis using the K2D2 algorithm of the CD spectrum indicated the following conformation: 23% α -helix, 24% β -sheet, and 53% coil (Table 3).

Analysis of the thermal melting of ECD2 protein as demonstrated that the ellipticity measured at 220 nm increased with increase in temperature, consistent with what would be expected to accompany protein unfolding in a α -helix to coil transition (Fig. 6A). In the temperature range of 20°C to 80°C, the plot for the wild-type ECD2 protein fitted well to a sigmoidal

curve (Fig. 6A inset) and the T_m was 49.8°C (Table 3). The thermal melting profile of the W1408L is shown in Fig. 6B. This mutant appeared more resistant to thermal denaturation than wtECD2, indicated by a T_m of 57.1°C (Table 3). Therefore, CD and thermal melting experiments suggest that the wild type and mutant polypeptides have relatively similar secondary structure compositions at 25°C, although a higher T_m may indicate a decreased structural flexibility.

C1488R Mutation - The C1488R mutation has been identified as a Stargardt disease-linked mutation in individuals of Northern and Central European ancestry (13,23,50). This mutation has been reported to occur in the ABCA4 gene as an individual heterozygous mutation as well as in trans with G863A mutation. This mutation represents a chemically significant substitution of a basic residue for a strictly conserved cysteine residue. The far-UV CD spectrum of C1488R mutant at 25°C is presented in Fig. 5. Nonlinear regression analysis of the CD spectrum using K2D2 algorithm indicated the following conformation: 20% α -helix, 27% β -sheet, and 53% coil (Table 3). Although a dramatic change in the overall CD spectrum of the protein was not observed, the substitution resulted in a significant alteration in the T_m , from 49.8°C to 66.7°C, as determined by thermal denaturation CD spectra (Fig. 6C & Table 3). The sudden increase in T_m of this mutant is not simply an indication of structural stability; rather it may signify loss of flexibility in the structure of this domain. A certain degree of structural flexibility may be important for its function. Introduction of the charged arginine residue at this location could lead to abnormal salt bridge formation, which would support this hypothesis.

R1443H Mutation - The R1443H mutation has been identified in individuals with Stargardt disease and appears to occur in those with Northern European as well as East Indian ancestry (23,54). From a biochemical perspective, Arg \rightarrow His represents a change from a highly basic residue, to an almost neutral residue, and thus represents a potentially significant change in terms of physico-chemical properties. The CD spectrum of this mutant was significantly altered (Fig. 5). Major shifts in the CD spectral minima at 208 and 220 nm for R1443H were observed at 25°C, consistent with a helix-coil transition concomitant

with a significant change of overall secondary structure (Fig. 5). Analysis of the spectra using the K2D2 method shows that the polypeptide had relatively little α -helical content, ~11%, as compared to 25% in wild-type ECD2 (Table 3). Comparing the spectra of the native and heat-denatured states of the R1443H mutant, it appears that the heat-induced alterations of the secondary structure elements over the temperature range of 20-80°C were small. It is likely that the absence of a sequential loss of structure with temperature may simply reflect the lack of α -helical structure of R1443H relative to wtECD2.

The ECD2 Domain Specifically Interacts with all-trans Retinal. ABCA4 is believed to function primarily in the transport and recycling of all-trans retinal produced in the ROS discs during the visual transduction cycle (55). The ECD2 domain may have a number of different roles in the function of ABCA4. Our hypothesis is that it may play a role in the interaction of ABCA4 with retinal. In this study, we had the opportunity to study the ECD2 domain separate from the rest of the ABCA4 molecule. Therefore, we have utilized this model system to examine ECD2 interaction with retinal. We observed a significant change in the tryptophan fluorescence emission spectrum of ECD2 protein upon retinal addition and the change was dose-dependent. We have used this as a fluorescence-based assay to investigate interaction of retinal derivatives with the ECD2 domain.

Inspection of the primary sequence of ECD2 shows that seven tryptophan residues are present in this domain. These residues provide an indicator of their surroundings as their fluorescence emission is attenuated in response to a shift from hydrophobic to hydrophilic environments as a consequence of conformational change (56). Changes in protein confirmation as a result of ligand binding or amino acid substitutions can thus be monitored. The fluorescence spectra of wild-type ECD2 polypeptide was collected at 25°C as described in “Experimental Procedures” in the absence and presence of all-trans retinal over a concentration range of 0-15 μ M. ECD2 displayed a strong emission maximum at 335 nm, characteristic of tryptophan residues in a hydrophobic environment (Fig 7A). Upon titration with all-trans retinal, the tryptophan emission maxima at 335 nm decreased in a dose-dependent manner and appeared to saturate at a concentration

of 10 μ M retinal (Fig 7A). We have examined fluorescence properties of all-trans retinal in the 300-400 nm range in order to examine the possibilities of inner-filter effects or fluorescence resonance energy transfer (FRET). All-trans retinal did not show any detectable absorption or emission in this wavelength range. These results indicated (1) the ECD2 polypeptide bound all-trans retinal, and (2) the binding accompanied concomitant conformational changes and/or changes in tryptophan environment. A semi-log plot of the attenuated fluorescence intensities at different all-trans retinal concentrations is shown in Fig. 8. The plot was fitted by non-linear regression using PRISM 5.0 to sigmoidal dose-response as detailed in “Experimental Procedures”. The K_d (or EC_{50}) was determined to be $1.3 \pm 1.1 \times 10^{-7}$ M for wild-type ECD2 protein.

In contrast to all-trans retinal, 11-cis retinal had only minor effects on the tryptophan emission spectrum of ECD2 in the same concentration range (Fig. 9). Although some changes with increasing concentrations of 11-cis retinal were observed, perturbations in the emission spectra were far less significant than that observed with all-trans retinal. Thus, either the binding of 11-cis retinal was far weaker than all-trans retinal or the binding of 11-cis retinal did not elicit the same extent of conformational changes as all-trans retinal binding. In either case, the effects of all-trans retinal are distinct from 11-cis retinal.

Our results indicated that all-trans retinal elicited a significant effect on the tryptophan emission spectrum of wild-type ECD2 protein. Therefore, we examined its effect on the tryptophan emission spectra of the three Stargardt mutants (Figs. 7B-D). Varying degrees of quenching of their intrinsic tryptophan fluorescence was observed in the presence of all-trans retinal, suggesting altered modes of binding in the mutants. With both W1408L and C1488R, attenuation of tryptophan fluorescence emission was observed with increasing concentrations of all-trans retinal (Fig. 7 B&C), albeit significantly diminished compared to that observed with the wild-type ECD2 (Figs. 7A). On the other hand, mutant Arg1443His displayed little change in tryptophan fluorescence spectra in the presence of all-trans retinal, which would indicate that this mutant did not undergo all-trans retinal binding

and/or associated conformational change. Quantitative analysis of all-*trans* retinal binding with these three ECD2 mutants is shown in Fig. 8. The K_d values for W1408L and C1488R were 8.1×10^{-7} M and 6.7×10^{-7} M, respectively. Compared to the wild-type ECD2, the binding of all-*trans* retinal by these mutants was significantly weaker. With R1433H mutant, the K_d value could not be determined and was estimated to be $>30 \mu\text{M}$.

Fluorescence Anisotropy Analysis of the Influence of the R1433H Mutation on all-trans Retinal Binding. Intrinsic tryptophan fluorescence analyses in the presence of all-*trans* retinal were indicative of conformational change, which in turn was suggestive of ECD2 protein-ligand interaction. Thus it was of interest to demonstrate direct binding of all-*trans* retinal to this domain. We have utilized fluorescence anisotropy analysis to evaluate all-*trans* retinal binding. Fluorescence anisotropy is normally used for direct measurements of ligand binding by determining the concentrations of bound and free ligand in solution due to differences in anisotropy values between bound and free ligand (44-45,57-58). Therefore, true equilibrium measurements are possible in this procedure without needing to isolate the protein•ligand complex from the free ligand. Due to its structural features, all-*trans* retinal is a natural fluorophore.

In order to determine the appropriate emission/excitation parameters to use in anisotropy studies, emission spectra of 100 nM all-*trans* retinal following excitation at 310 nm were collected over the range 370-570 nm. All-*trans* retinal displayed an emission maximum at 430 nm (Fig. 10A) and thus anisotropy was measured using 100 nM all-*trans* retinal with the wavelengths set at 310 nm for excitation and 430 nm for emission. The fluorescence anisotropy changes with ECD2 protein concentration are shown in Fig. 10B. For wild-type ECD2 protein, a sigmoidal semilog plot was obtained indicating equilibrium saturation binding of all-*trans* retinal by this protein. Clearly, the binding of the R1433H mutant was impaired relative to that of the wild type protein, as indicated by its inability to achieve saturation. The plots, shown in Fig. 10B, were generated by nonlinear regression analysis of the data using commercial graphing software (PRISM, GraphPad Inc.). The binding

parameters were determined from the fluorescence anisotropy data by equilibrium binding analysis and fitted to Equation 3, using the BIOEQS program (45). This nonlinear regression analysis gave a dissociation constant (K_D) for ECD2 of $4.0 \pm 1.3 \times 10^{-7}$ M for the wild type protein.

DISCUSSION

The ABCA4 protein is an essential component of the visual signal transduction cycle in rod and cone cells of vertebrate retina. Currently no direct assay for measurement of ABCA4 mediated transport is available. However, ABCA4 knock-out mice, as well as patients harboring mutations in ABCA4, display accumulation of all-*trans* retinal and N-retinylidene-PE in rod photoreceptor disc membranes, providing evidence that ABCA4 protein functions in the recycling of all-*trans* retinal (20,59-60). ABCA4 contains two extended extracellular loops that are evolutionarily conserved but lack any apparent function. Genetic studies involving patients with inherited macular degenerations, demonstrate mutations in these domains clearly impair ABCA4 transporter function, thereby establishing important role(s) of the ECDs (19,23,50-51,54).

The Second Extracellular Domain of ABCA4 Possesses a Highly Ordered and Stable Conformation. In order to delineate its role in ABCA4 transporter function, we first explored the structure and conformational features of the ECD2 domain and alterations due to disease-associated mutations. Analysis of the CD spectral data using the K2D2 method indicated that the wild type polypeptide possessed a highly ordered structure that has a reasonably high α -helical content in addition to β -sheet and extended structures. Depending on the mutation, ECD2 protein conformation changed only slightly or very drastically. Thus, CD analysis provided a method for monitoring conformational changes due to macular degenerative disease associated mutations.

Unfortunately despite an intensive search, very little collective information correlating the severity and age of onset with a given mutation is available, making it difficult for us to correlate the observed structural defects with a given clinical phenotype.

Influence of Stargardt Disease Associated Mutations on ECD2 Domain Secondary Structure:

Of the three mutants examined here, the R1443H mutation appeared to be the most severe in terms of its influence on the secondary structure of ECD2. As a consequence of this mutation, the ECD2 polypeptide appeared to lose the majority of its α -helical secondary structure (Fig. 5). Very little change was observed in the protein's structure in response to temperature (Fig. 6D), suggesting that the polypeptide was highly disordered. A minimal change in the CD spectrum was observed with the W1409L mutation. This mutant appeared to have secondary structural parameters which were comparable to that of the wild type ECD2 polypeptide. In addition, only a small increase in T_m was observed from the thermal melting curves. This small increase may be due to the decrease in relative hydrophobicity associated with the W \rightarrow L mutation, such as that described by Kotik and coworkers in their studies which examining the role of tryptophan residues in the structural and thermal stability of lactate dehydrogenase (61). The C1488R mutation appeared to be intermediate in nature with respect to its influence on the ECD2 structure. Based on the CD analysis of the protein, it appeared to have lower α -helix content. Interestingly, a major increase in the T_m obtained from the thermal melting profile of the CD spectra was observed. The substitution of a charged residue, arginine for cysteine, may provide enhanced thermal stability to the structure, perhaps through ionic interactions. Liao and coworkers report similar increases in T_m upon introduction of charged residues into porcine $\alpha\beta$ -crystallin (62). *ECD2 Domain Interacts Specifically with all-trans Retinal:* Several lines of investigation support the hypothesis that all-trans retinal, the product of the visual transduction cycle, is the substrate of ABCA4 (63-65). Physiologically, studies of ABCA4 knockout mice show elevated levels of all-trans retinal and the protonated Schiff's base, N-retinylidene-PE, as well as the di-retinal pyridinium compound A2E in the retinal pigment epithelium (65-67). Together these studies strongly support all-trans retinal as the substrate for ABCA4. However, at present no assay for ATP dependent transport by ABCA4 has been developed and which region of the ABCA4 molecule interacts specifically with the substrate remains to be identified.

Using tryptophan fluorescence emission spectrum, we have investigated the binding of ECD2 domain to retinal, and examined how this binding is affected in disease associated mutants. When all-trans retinal was added to ECD2 polypeptide, dose-dependent attenuation of its tryptophan fluorescence was observed (Fig. 7). Titration with all-trans retinal was used to evaluate the binding quantitatively, and the ECD2 polypeptide bound all-trans retinal with reasonably high affinity, $K_{d, app}$ of 1.3×10^{-7} M (Fig. 8 and Table 3). The binding appeared highly specific as attenuation of tryptophan fluorescence by 11-cis retinal was significantly lower (Fig 9). The affinity of interaction for all-trans retinal observed in our experimental system is approximately ~30-fold higher than that previously reported by Beharry et al. (64). Using fluorescence anisotropy we were able to demonstrate direct interaction of the ECD2 polypeptide and quantitate its interaction. The K_D of $4 \pm 1.3 \times 10^{-7}$ is approximately 2-fold higher than that derived from the intrinsic tryptophan fluorescence. This small difference may be attributed to the fact that the two approaches are assessing retinal interaction through the measurement of two different parameters: one examines the change in ECD2 protein structure as using tryptophan environment as a reporter, the other approach measuring the fluorescence anisotropy of all-trans retinal itself.

The locations of the seven tryptophan residues are indicated on the multiple sequence alignment shown in Figure 2. These residues are strictly conserved and are distributed across the domain. The emission maxima and quantum yields of tryptophan residues vary widely between proteins and can be a function of protein structure (37{Lugo, 2009 #4375{Lakowicz, 2006 #1086}). A given protein conformation may contribute to specific protein environments that quench a given tryptophan residue or residues. All-trans retinal is a relatively large, hydrophobic molecule and its binding site would need to be hydrophobic as well. Indeed, studies examining retinoid binding properties of the nematode ABA-1 allergen protein, describe the major structural role of tryptophan in providing a hydrophobic binding site for the ligand (68). A possible explanation for the observed decrease in fluorescence would be that the ECD2 domain undergoes a conformational

change during retinal binding, in order to create a hydrophobic pocket. The conformational change causes a change in the environment of the tryptophan residues, thereby leading to the observed decrease in fluorescence. This

These studies indicate that the ECD2 domain is involved in binding all-*trans* retinal in its transport across the ROS disc membrane. ECD2 may also be involved in the transport of retinal derivatives, such as N-retinylidene-phosphatidyl ethanolamine, since the Schiff's base present in these compounds is formed from the aldehyde functional group of all-*trans* retinal.

Influence of Stargardt Disease Associated Mutations on ECD2 Interaction with all-trans Retinal: To date the biochemical observables measured for mutant ABCA4 proteins have been restricted to ATP binding and hydrolysis; protein localization of heterologously expressed protein in cell culture, and interaction of the nucleotide binding domains (32,67,69-72). All mutants investigated demonstrated decreases in their affinity of interaction with all-*trans* retinal, based on their ability to attenuate intrinsic tryptophan fluorescence (Figs. 7 & 8). In the case of mutant R1443H a large decrease in the binding affinity was observed, with a >250-fold increase in K_d (Fig. 8 and Table 3). Less dramatic changes were seen with the other mutants investigated in this study; with a 5-8-fold increase in K_d for W1408L and C1488R respectively. With mutant R1443H, apparent lack of interaction with all-*trans* retinal was observed. Direct analysis of mutant R1433H interaction confirmed impairment of all-*trans* retinal binding by this mutant, as shown by the inability to achieve saturation (Fig. 10B). Interestingly, the functional alterations in all-*trans* retinal interaction were mirrored by the structural alterations in this domain as determined by CD spectroscopic analysis of their conformations. The conformation of R1443H was strikingly different from that of wt ECD2, and appeared refractory to changes in temperature. It is likely that its inability to interact with all-*trans* retinal has a basis in its abnormal structural features. Likewise, the relatively moderate structural changes of W1408L and C1488R also correlated with more moderate changes in interaction with all-*trans* retinal as compared to the wild type ECD2.

This report demonstrates that the ECD2 domain of ABCA4 has a highly ordered and stable

secondary structure, which appears to undergo conformational change in response to its specific interaction with its putative substrate all-*trans* retinal. Disease associated mutations in this domain were observed to influence the secondary structure and all-*trans* retinal binding affinity. Further studies of each of the ABCA4 domains are required to elucidate the mechanism of retinal transport by this complex and physiologically important ABC transporter.

REFERENCES

1. Higgins, C. F. (1992) *Annu Rev Cell Biol* **8**, 67-113
2. Higgins, C. F. (2001) *Res Microbiol* **152**, 205-210
3. Higgins, C. F., and Linton, K. J. (2001) *Science* **293**, 1782-1784
4. Hettema, E. H., van Roermund, C. W., Distel, B., van den Berg, M., Vilela, C., Rodrigues-Pousada, C., Wanders, R. J., and Tabak, H. F. (1996) *Embo J* **15**, 3813-3822
5. Ewart, G. D., Cannell, D., Cox, G. B., and Howells, A. J. (1994) *J Biol Chem* **269**, 10370-10377
6. Ewart, G. D., and Howells, A. J. (1998) *Methods Enzymol* **292**, 213-224
7. Berkower, C., and Michaelis, S. (1991) *Embo J* **10**, 3777-3785
8. Walker, J. E., Saraste, M., Runswick, M. J., and Gray, N. (1982) *EMBO J.* **1**, 945-951
9. Dean, M., Rzhetsky, A., and Allikmets, R. (2001) *Genome Res* **11**, 1156-1166
10. Illing, M., Molday, L. L., and Molday, R. S. (1997) *J Biol Chem* **272**, 10303-10310
11. Papermaster, D. S., Schneider, B. G., Zorn, M. A., and Kraehenbuhl, J. P. (1978) *J. Cell. Biol.* **78**, 415-425
12. Allikmets, R. (2000) *Am J Hum Genet* **67**, 487-491
13. Briggs, C. E., Rucinski, D., Rosenfeld, P. J., Hirose, T., Berson, E. L., and Dryja, T. P. (2001) *Invest Ophthalmol Vis Sci* **42**, 2229-2236
14. Klevering, B. J., Blankenagel, A., Maugeri, A., Cremers, F. P., Hoyng, C. B., and Rohrschneider, K. (2002) *Invest Ophthalmol Vis Sci* **43**, 1980-1985
15. Klevering, B. J., Deutman, A. F., Maugeri, A., Cremers, F. P., and Hoyng, C. B. (2005) *Graefes Arch Clin Exp Ophthalmol* **243**, 90-100
16. Zhang, K., Kniazeva, M., Hutchinson, A., Han, M., Dean, M., and Allikmets, R. (1999) *Genomics* **60**, 234-237
17. Allikmets, R., Singh, N., Sun, H., Shroyer, N. F., Hutchinson, A., Chidambaram, A., Gerrard, B., Baird, L., Stauffer, D., Peiffer, A., Rattner, A., Smallwood, P., Li, Y., Anderson, K. L., Lewis, R. A., Nathans, J., Leppert, M., Dean, M., and Lupski, J. R. (1997) *Nat Genet* **15**, 236-246
18. Arnell, H., Mantyjarvi, M., Tuppurainen, K., Andreasson, S., and Dahl, N. (1998) *Acta Ophthalmol Scand* **76**, 649-652
19. Fishman, G. A., Stone, E. M., Grover, S., Derlacki, D. J., Haines, H. L., and Hockey, R. R. (1999) *Arch Ophthalmol* **117**, 504-510
20. Molday, R. S. (2007) *J Bioenerg Biomembr* **39**, 507-517
21. Bennett, J. (2009) *N Engl J Med* **361**, 2483-2484
22. Simonelli, F., Maguire, A. M., Testa, F., Pierce, E. A., Mingozi, F., Bennicelli, J. L., Rossi, S., Marshall, K., Banfi, S., Surace, E. M., Sun, J., Redmond, T. M., Zhu, X., Shindler, K. S., Ying, G. S., Ziviello, C., Acerra, C., Wright, J. F., McDonnell, J. W., High, K. A., Bennett, J., and Auricchio, A. (2009) *Mol Ther*
23. Jaakson, K., Zernant, J., Kulm, M., Hutchinson, A., Tonisson, N., Glavac, D., Ravnik-Glavac, M., Hawlina, M., Meltzer, M. R., Caruso, R. C., Testa, F., Maugeri, A., Hoyng, C. B., Gouras, P., Simonelli, F., Lewis, R. A., Lupski, J. R., Cremers, F. P., and Allikmets, R. (2003) *Hum Mutat* **22**, 395-403
24. Bungert, S., Molday, L. L., and Molday, R. S. (2001) *J Biol Chem* **276**, 23539-23546
25. Yatsenko, A. N., Wiszniewski, W., Zaremba, C. M., Jamrich, M., and Lupski, J. R. (2005) *J Mol Evol* **60**, 72-80
26. Chen, W., and Bahl, O. P. (1993) *Mol Cell Endocrinol* **91**, 35-41
27. Zhang, G., Xi, J., Wang, X., Guo, J., Zhang, H., Yang, Y., Qiao, S., Wang, L., He, L., and Zhu, Y. (2008) *J Immunol Methods* **334**, 21-28

28. Ling, V. (1997) *Cancer Chemother Pharmacol* **40 Suppl**, S3-8
29. Duffieux, F., Annereau, J. P., Boucher, J., Miclet, E., Pamard, O., Schneider, M., Stoven, V., and Lallemand, J. Y. (2000) *Eur J Biochem* **267**, 5306-5312
30. Biswas, E. E. (2001) *Biochemistry* **40**, 8181-8187
31. Biswas-Fiss, E. E. (2003) *Biochemistry* **42**, 10683-10696.
32. Suarez, T., Biswas, S. B., and Biswas, E. E. (2002) *J Biol Chem* **277**, 21759-21767
33. Massiah, M. A., Ko, Y.-H., Pederson, P. L., and Mildvan, A. S. (1999)
34. Sheppard, D. N., and Welsh, M. J. (1999) *Physiol Rev* **79**, S23-45
35. Kreimer, D. I., Malak, H., Lakowicz, J. R., Trakhanov, S., Villar, E., and Shnyrov, V. L. (2000) *Eur J Biochem* **267**, 4242-4252
36. Sambrook, J., Fritsch, E.F. and Maniatis, T. (1989) *Molecular Cloning: A Laboratory Manual*, Cold Spring Harbor Press, Cold Spring Harbor, NY
37. Winterfeld, S., Imhof, N., Roos, T., Bar, G., Kuhn, A., and Gerken, U. (2009) *Biochemistry* **48**, 6684-6691
38. Booth, C. L., Pulaski, L., Gottesman, M. M., and Pastan, I. (2000) *Biochemistry* **39**, 5518-5526
39. Balan, A., Ferreira, R. C., and Ferreira, L. C. (2008) *Genet Mol Res* **7**, 117-126
40. Brunkhorst, C., Wehmeier, U. F., Piepersberg, W., and Schneider, E. (2005) *Res Microbiol* **156**, 322-327
41. Mace, P. D., Cutfield, J. F., and Cutfield, S. M. (2007) *Protein Expr Purif* **52**, 40-49
42. Perez-Iratxeta, C., and Andrade-Navarro, M. A. (2008) *BMC Struct Biol* **8**, 25
43. Andrade, M. A., Chacon, P., Merelo, J. J., and Moran, F. (1993) *Protein Eng* **6**, 383-390
44. Boyer, M., Poujol, N., Margeat, E., and Royer, C. A. (2000) *Nucleic Acids Res.* **28**, 2494-2502
45. Ozers, M. S., Hills, J. J., Ervin, K., Wood, J. R., Nardulli, A. M., Royer, C. A., and Gorski, J. (1997) *J. Biol. Chem.* **272**, 30405-30411
46. Ozers, M. S., Hill, J. J., Ervin, K., Wood, J. R., Nardulli, A. M., Royer, C. A., and Gorski, J. (1997) *J Biol Chem* **272**, 30405-30411
47. Bradford, M. M. (1976) *Anal Biochem* **72**, 248-254
48. Laemmli, U. K. (1970) *Nature* **227**, 680-685
49. Kyte, J., and Doolittle, R. F. (1982) *J Mol Biol* **157**, 105-132
50. Lewis, R. A., Shroyer, N. F., Singh, N., Allikmets, R., Hutchinson, A., Li, Y., Lupski, J. R., Leppert, M., and Dean, M. (1999) *Am J Hum Genet* **64**, 422-434
51. Webster, A. R., Heon, E., Lotery, A. J., Vandenburg, K., Casavant, T. L., Oh, K. T., Beck, G., Fishman, G. A., Lam, B. L., Levin, A., Heckenlively, J. R., Jacobson, S. G., Weleber, R. G., Sheffield, V. C., and Stone, E. M. (2001) *Invest Ophthalmol Vis Sci* **42**, 1179-1189
52. Fishman, G. A., Stone, E.M., Eilason, D.A., Taylor, C.M., Lindeman, M. and Derlacki, D.J. (2003) *Ophthalmic Molecular Genetics* **121**, 851-855
53. Samanta, U., and Chakrabarti, P. (2001) *Protein Eng* **14**, 7-15
54. September, A. V., Vorster, A. A., Ramesar, R. S., and Greenberg, L. J. (2004) *Invest Ophthalmol Vis Sci* **45**, 1705-1711
55. Molday, R. S., Zhong, M., and Quazi, F. (2009) *Biochim Biophys Acta* **1791**, 573-583
56. Lakowicz, J. R. (1999) *Principals of Fluorescence Spectroscopy*, 2nd Edition ed., Kluwer Academic/Plenum Publishers
57. Nahoum, V., Perez, E., Germain, P., Rodriguez-Barrios, F., Manzo, F., Kammerer, S., Lemaire, G., Hirsch, O., Royer, C. A., Gronemeyer, H., de Lera, A. R., and Bourguet, W. (2007) *Proc Natl Acad Sci U S A* **104**, 17323-17328
58. Pogenberg, V., Guichou, J. F., Vivat-Hannah, V., Kammerer, S., Perez, E., Germain, P., de Lera, A. R., Gronemeyer, H., Royer, C. A., and Bourguet, W. (2005) *J Biol Chem* **280**, 1625-1633

59. Saari, J. C. (2000) *Invest Ophthalmol Vis Sci* **41**, 337-348
60. Lamb, T. D., and Pugh, E. N., Jr. (2006) *Invest Ophthalmol Vis Sci* **47**, 5137-5152
61. Kotik, M., and Zuber, H. (1993) *Eur J Biochem* **211**, 267-280
62. Liao, J. H., Lee, J. S., Wu, S. H., and Chiou, S. H. (2009) *Mol Vis* **15**, 1429-1444
63. Ahn, J., and Molday, R. S. (2000) *Methods Enzymol* **315**, 864-879
64. Beharry, S., Zhong, M., and Molday, R. S. (2004) *J Biol Chem* **279**, 53972-53979
65. Weng, J., Mata, N. L., Azarian, S. M., Tzekov, R. T., Birch, D. G., and Travis, G. H. (1999) *Cell* **98**, 13-23
66. Radu, R. A., Mata, N. L., Bagla, A., and Travis, G. H. (2004) *Proc Natl Acad Sci U S A* **101**, 5928-5933
67. Sun, H., Molday, R. S., and Nathans, J. (1999) *J Biol Chem* **274**, 8269-8281
68. Kennedy, M. W., Brass, A., McCrudden, A. B., Price, N. C., Kelly, S. M., and Cooper, A. (1995) *Biochemistry* **34**, 6700-6710
69. Ahn, J., Wong, J. T., and Molday, R. S. (2000) *J Biol Chem* **275**, 20399-20405
70. Biswas-Fiss, E. E. (2003) *Biochemistry* **42**, 10683-10696
71. Biswas-Fiss, E. E. (2006) *Biochemistry* **45**, 3813-3823
72. Shroyer, N. F., Lewis, R. A., Yatsenko, A. N., Wensel, T. G., and Lupski, J. R. (2001) *Hum Mol Genet* **10**, 2671-2678

FOOTNOTES

The authors would like to thank Drs. Richard Lewis (Baylor College of Medicine; Houston, TX) and Rando Allikmets (Columbia University; New York, NY) for additional insights regarding the clinical phenotypes of patients harboring ABCA4 mutations, and Drs. Robert Molday (University of British Columbia, Canada) and S. Biswas (UMDNJ, Stratford, NJ) for helpful discussions. The authors are also grateful Dr. S. Greening (Thomas Jefferson University) for editorial review of the manuscript. Portions of this work were completed by Kinjalben Joshi in partial satisfaction of the MS in Bioscience Technologies (Biotechnology track) degree requirements at Thomas Jefferson University. This work was supported by a grant from the National Institutes of Health, National Eye Institute, EY 013113, and an NIH administrative supplement, Quantitative Physical Measurements at the Nanaoscale to EEB-F.

The abbreviations used are: ABC, ATP binding cassette, TMD, Transmembrane domain; Tris, tris (hydroxymethyl) aminomethane; BSA, bovine serum albumin; EDTA, ethylenediaminetetraacetic acid; ATP, adenosine triphosphate; ATPase, adenosine triphosphatase; ECD, extra cellular domain; NBD, nucleotide binding domain; ABCA4, retina specific ABC transporter; ROS, rod outer segment; STGD1, Stargardt disease, arCRD, autosomal recessive Cone-Rod Dystrophy, AMD, Age-Related Macular Degeneration; CD, circular dichroism.

FIGURE LEGENDS

Fig. 1. Predicted Structural Organization of ABCA4 and Its Domains. Pictorial representation showing the cytoplasmic, extracellular and transmembrane domains of ABCA4 protein. The domains were defined based on current topological models of ABCA4 (24), and are as follows: NDB1 aa 854 - 1375, NBD2 aa 1898-2273, ECD1 aa 62-646 and ECD2 aa 1395-1680.

Fig. 2. Sequence Alignment of ECD2 Domains of ABCA4 Proteins Derived from Several Vertebrate Species. The amino acid sequences of several vertebrate organisms were obtained from NCBI; *H. sapiens* (human), *M. faccicularis* (crab eating macaque), *B. taurus* (bovine), *C. familiaris* (dog), *M. musculus* (mouse) and *X. laevis* (African clawed frog), and were aligned using ClustalW. The amino acid residue number for each protein is indicated at the beginning of

each sequence. The alignment is color coded to indicate chemical characteristics of a given amino acid: red, basic; blue hydrophobic; green, hydrophilic; orange, neutral, pink, acidic, and light green, proline. Missense mutations examined in this study are enclosed by boxes.

Fig. 3. Purification of ABCA4-ECD2 Protein. (A) Overexpression of ABCA4-ECD2 Polypeptide. SDS-PAGE analysis of the overexpressed ECD2 polypeptide in *E. coli*. Expression of the recombinant protein was carried out as described in “Methods” in the presence of 0.25 mM IPTG. Equal amounts of cells before and after induction were analyzed. Lane 1, protein molecular mass standard; lane 2, uninduced RIPL (DE3)/pET30b ECD2 cell lysate; and lane 3, cell lysate from IPTG induced RIPL (DE3)/pET30b ECD2. (B) ECD2 Polypeptide Purified by S-Protein Agarose Chromatography. SDS-PAGE of S-protein agarose purification of ECD2. An aliquot (corresponding to 10 μ g) of purified ECD2 was analyzed on a 5 \rightarrow 18% SDS PAGE gel which was stained with Coomassie Blue R250 following electrophoresis. (C) ECD2 Wild Type and Mutant Purified Refolded Polypeptides. Approximately 4.5 μ g of the respective purified, refolded protein was loaded onto a 5–18% SDS-PAGE, which was stained with Coomassie Blue R-250 following electrophoresis. As shown the ABCA4-ECD2 protein migrated with predicted molecular mass of ~34 kDa.

Fig. 4. Circular Dichroism Spectra of Native and Refolded ABCA4-ECD2 Polypeptides. Comparative far-UV (200-250 nm) CD spectra of ECD2 from S-tag agarose and refolding-based purifications. The concentration of ECD2 polypeptide was 10 μ M in 10 mM NaPO₄, pH 7.5, 100 mM NaCl. The spectra were acquired with a 5 mm path length cuvette, at 25°C; scans were collected five times and averaged. Buffer spectra were always subtracted. Native-S-protein agarose chromatography (dashed line), refolded (solid line).

Fig. 5. Circular Dichroism Spectra of Wild Type and Mutant ABCA4-ECD2 Polypeptides. CD spectra were collected from highly purified homogenous preparations of recombinant wild type and mutant ECD2 polypeptides. Far-UV (200-250 nm) CD spectra were acquired with a 5 mm path length cuvette. The concentration of ECD2 polypeptides were 10 μ M in 10 mM KPO₄, pH 7.5, 100 mM NaCl. The spectra were acquired with a 5 mm path length cuvette, at 25°C; scans were collected five times and averaged. Buffer spectra were always subtracted.

Fig. 6. Circular Dichroism Spectra of Wild Type and Mutant ABCA4-ECD2 Polypeptides as a Function of Temperature. CD spectra were acquired (200-250 nm) over the range of 20-80°C, at 10°C increments, using a resolution of 0.2°C. The concentration of ECD2 wild type and mutant polypeptides were 10 μ M in 10 mM NaPO₄, pH 7.5, 100 mM NaCl. The spectra were acquired with a 5 mm path length cuvette, at 25°C; scans were collected five times and averaged. Buffer spectra were always subtracted. (A) wild type ECD2; inset: ellipticity at 220 nm was monitored over the range of 20-80°C and the T_m was determined from the inflection points of data fitted to sigmoidal curve.; (B) W1408L; (C) C1488R, and (D) R1443H.

Fig. 7. Tryptophan Fluorescence Intensity of Wild-Type and Mutant ABCA4-ECD2 Polypeptides in the Presence of all-*trans* Retinal. Fluorescence spectra of wild-type and mutant ECD2 polypeptides were collected at 25°C in the presence of increasing amounts of all-*trans* retinal over the concentration range 0-15 μ M as indicated. The concentration of ECD2 polypeptide was 3 μ M in 10 mM NaPO₄, pH 7.5, 100 mM NaCl. The scans were conducted in triplicate and the data were analyzed by least-squares regression analysis using Graph Pad PRISM software.

Fig. 8. Ligand Binding Analysis by Monitoring Changes in Intrinsic Tryptophan Fluorescence in the Presence of all-*trans* Retinal. Data obtained from the fluorescence spectra of wild-type and mutant ECD2 polypeptides described in Figure 7 were analyzed in terms of percent change in intensity versus log of the all-*trans* retinal concentration. (★) ECD2 WT; (▼) R1443H; (■) W1408L; (◇) C1488R.

Fig. 9. Tryptophan Fluorescence Intensity of Wild-Type ECD2 in the Presence of 11-*cis* Retinal. Fluorescence spectra of wild-type ECD2 polypeptide were collected at 25°C in the presence of increasing amounts of 11-*cis* retinal over the concentration range 0-10 µM as indicated. The concentration of ECD2 polypeptide was 3 µM in 10 mM NaPO₄, pH 7.5, 100 mM NaCl. The scans were conducted in triplicate and the data were analyzed by least-squares regression analysis using Graph Pad PRISM software.

Fig. 9. Fluorescence Anisotropy Analysis of ECD2 proteins with the all-*trans* Retinal. (A) Emission spectrum of 100 nM all-*trans* retinal (ATR). Excitation was 310 nm and emission was scanned over a range of 370 to 570 nm (B) Anisotropy titrations using wild-type ECD2 (○) and the R1433H mutant (◇). The titrations were carried out as described under “Materials and Methods.” Fluorescence anisotropy measurements were collected for ATR•ECD2 protein samples formed by the stepwise addition of ECD2 protein to 100 nM ATR. All samples were incubated at room for 2–3 min with constant stirring before taking anisotropy measures. The data were fitted with BIOEQS using a simple binding model (monomer) for all-*trans* retinal binding to wild-type and R1433H proteins NBD1 proteins.

Table 1: Stargardt Disease Associated Mutations Occurring in the ECD2 Domain Investigated in this Study.

Mutation	Base Change	Mutagenesis Primer
R1443H	<u>CG</u> C4328 <u>CAC</u>	5'-CAGGCTTTGGCAACCACTGAAGGAAGGGTGGCTTC-3'
W1408L	T <u>GG</u> 4221 <u>TTG</u>	5'-ACCCTTCACCCCTTGATATGGGCAGCAGTACACCTTC-3'
C1488R	<u>TGC</u> 4462 <u>CGC</u>	5'-AACCTTCACCATCCCGCAGGTGCAGCACCAGGGAGAAG-3'

Table 2: Summary of the Secondary Structure for ECD2 Polypeptide.

Secondary Structure ECD2 protein	α-helix	β-sheet	Extended-coil
Affinity Purified	0.27	0.20	0.53
Refolded	0.25	0.20	0.55

Table 3: Summary of Secondary Structure Analysis and Binding Constants for the ABCA4-ECD2 WT and Mutant Polypeptides Based on CD Data Analyzed by K2D2 Method (42-43).

Genotype	α-helix	β-sheet	Random coil	T_m (°C)	K_d (M)
Wild-type	0.25	0.20	0.55	49.7	1.3 x 10 ⁻⁷
R1433H	0.11	0.39	0.50	n.d.	n.d.
W1408L	0.23	0.24	0.53	57.1	8.1 x 10 ⁻⁷
C1488R	0.20	0.27	0.53	66.7	6.7 x 10 ⁻⁷

FIGURE 1

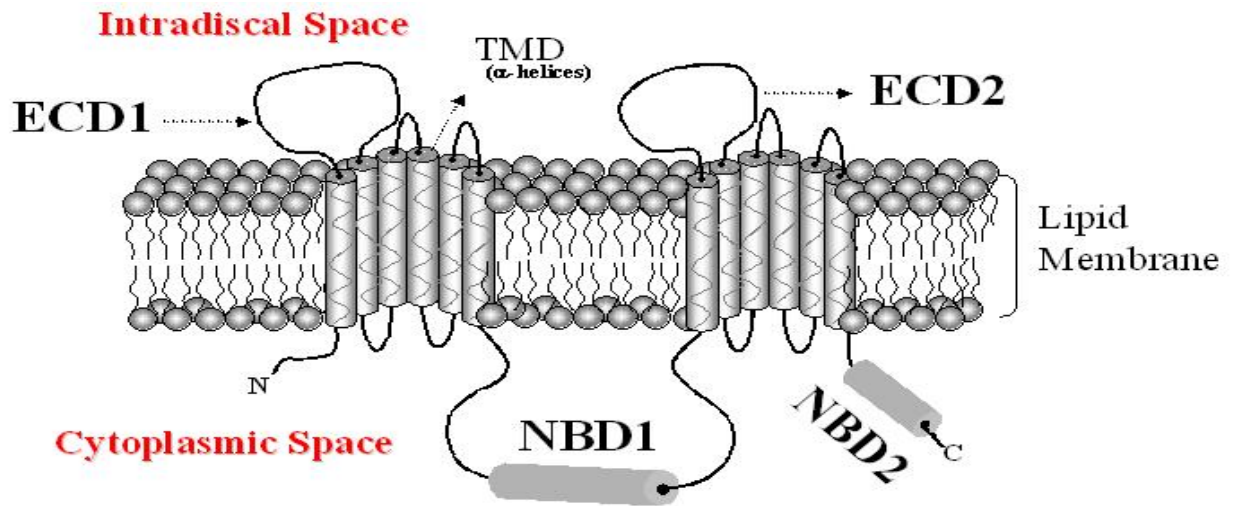


FIGURE 2

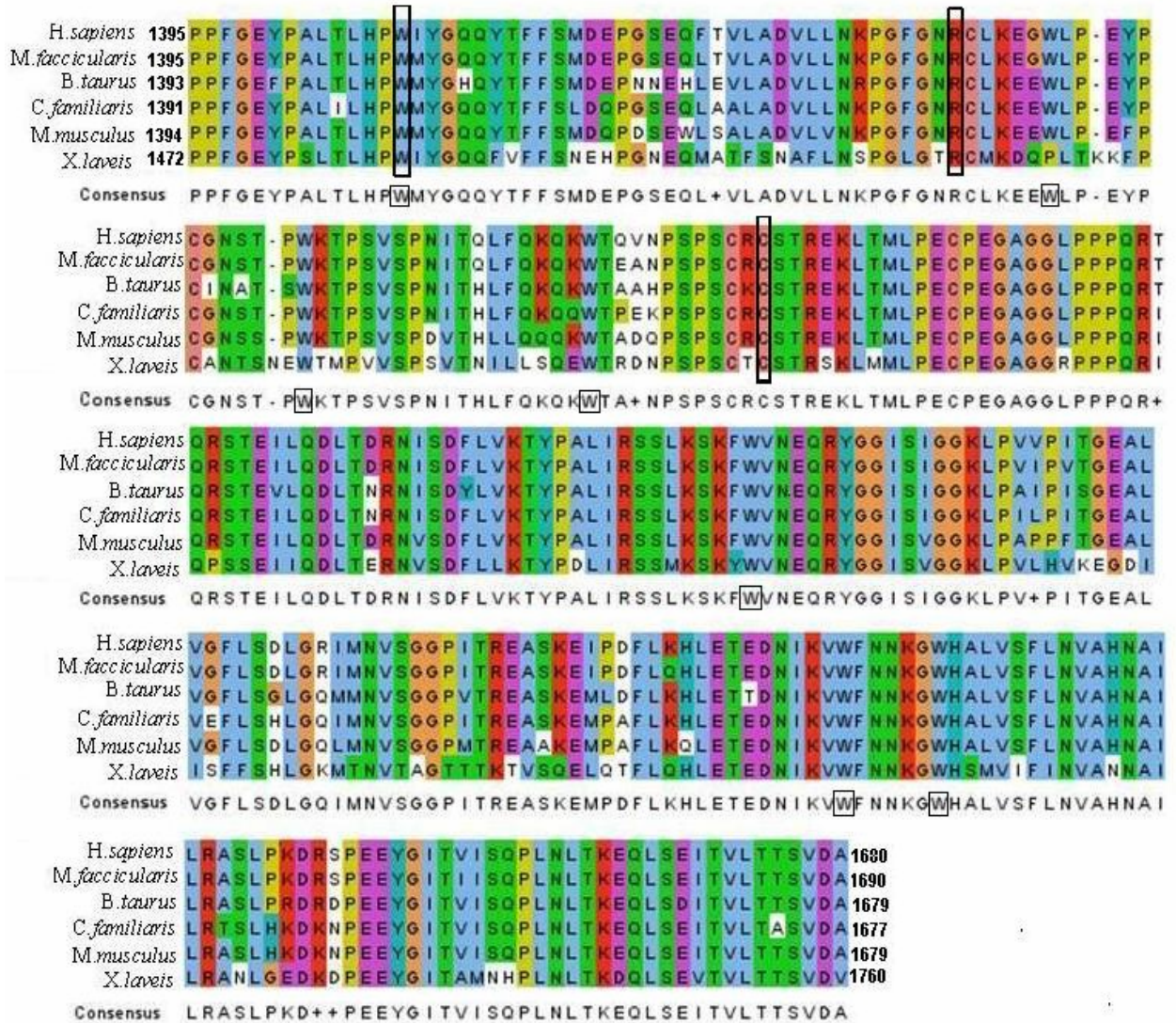


FIGURE 3

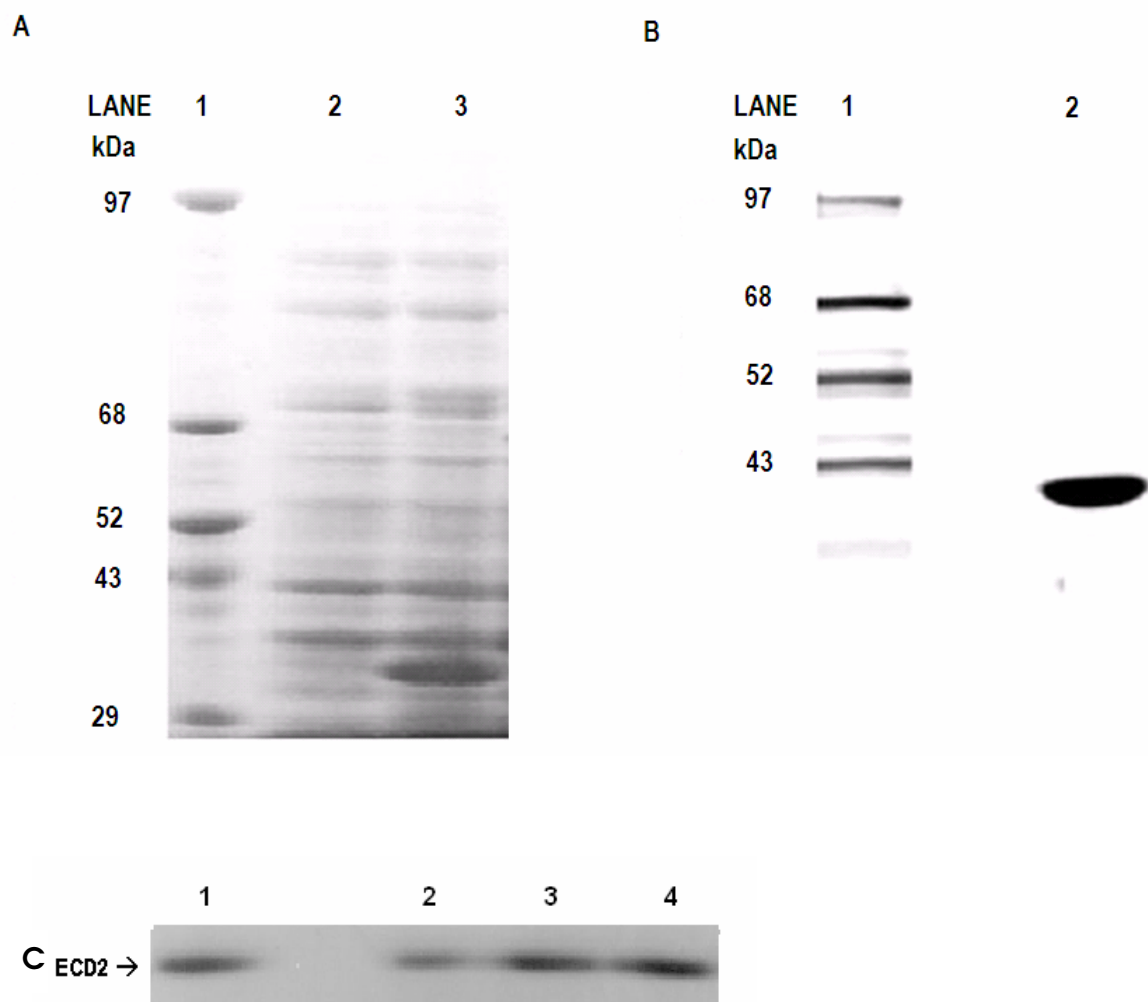


FIGURE 4

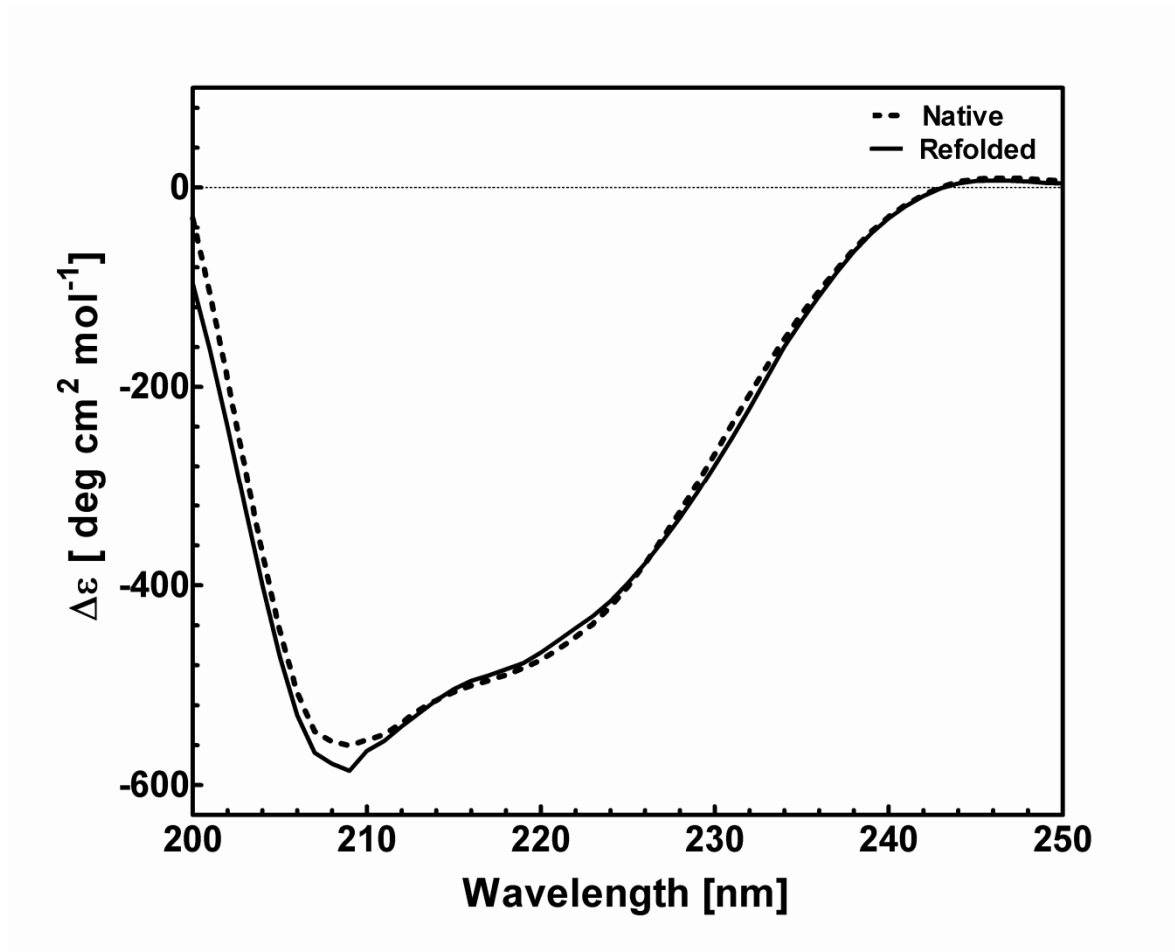


FIGURE 5

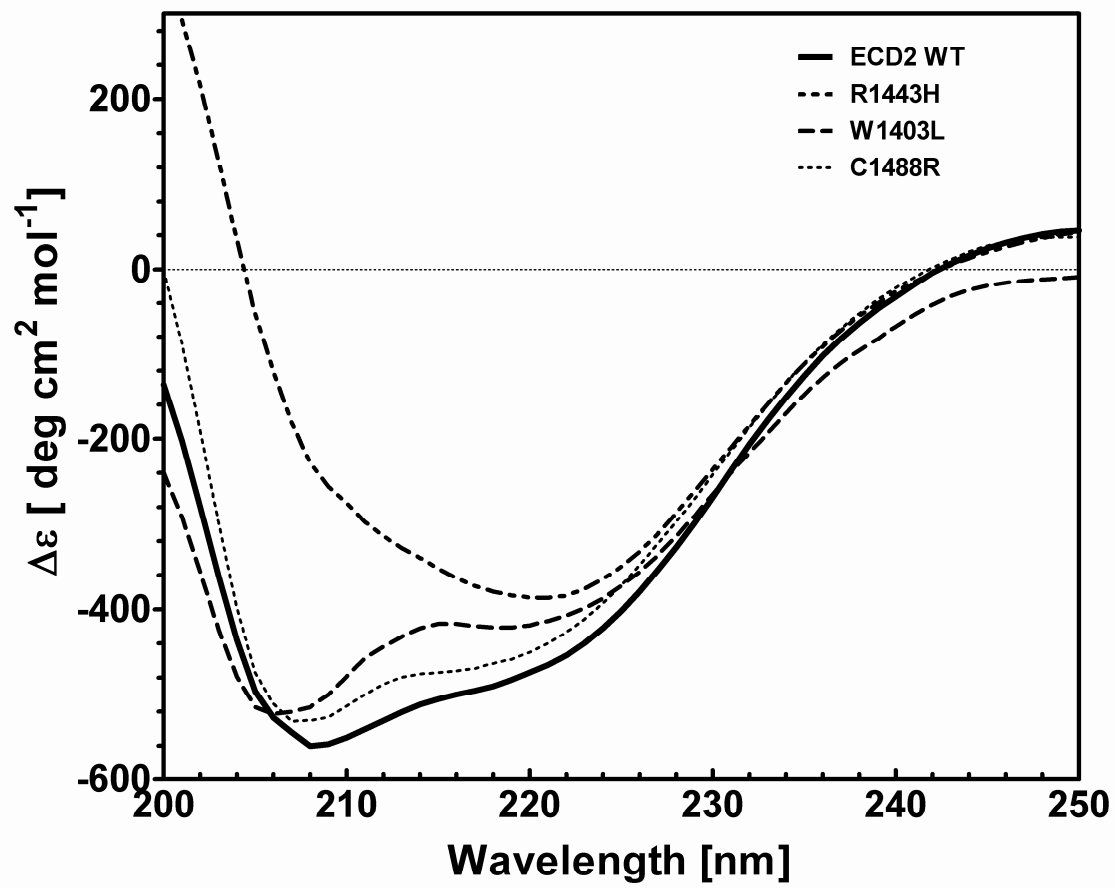


FIGURE 6

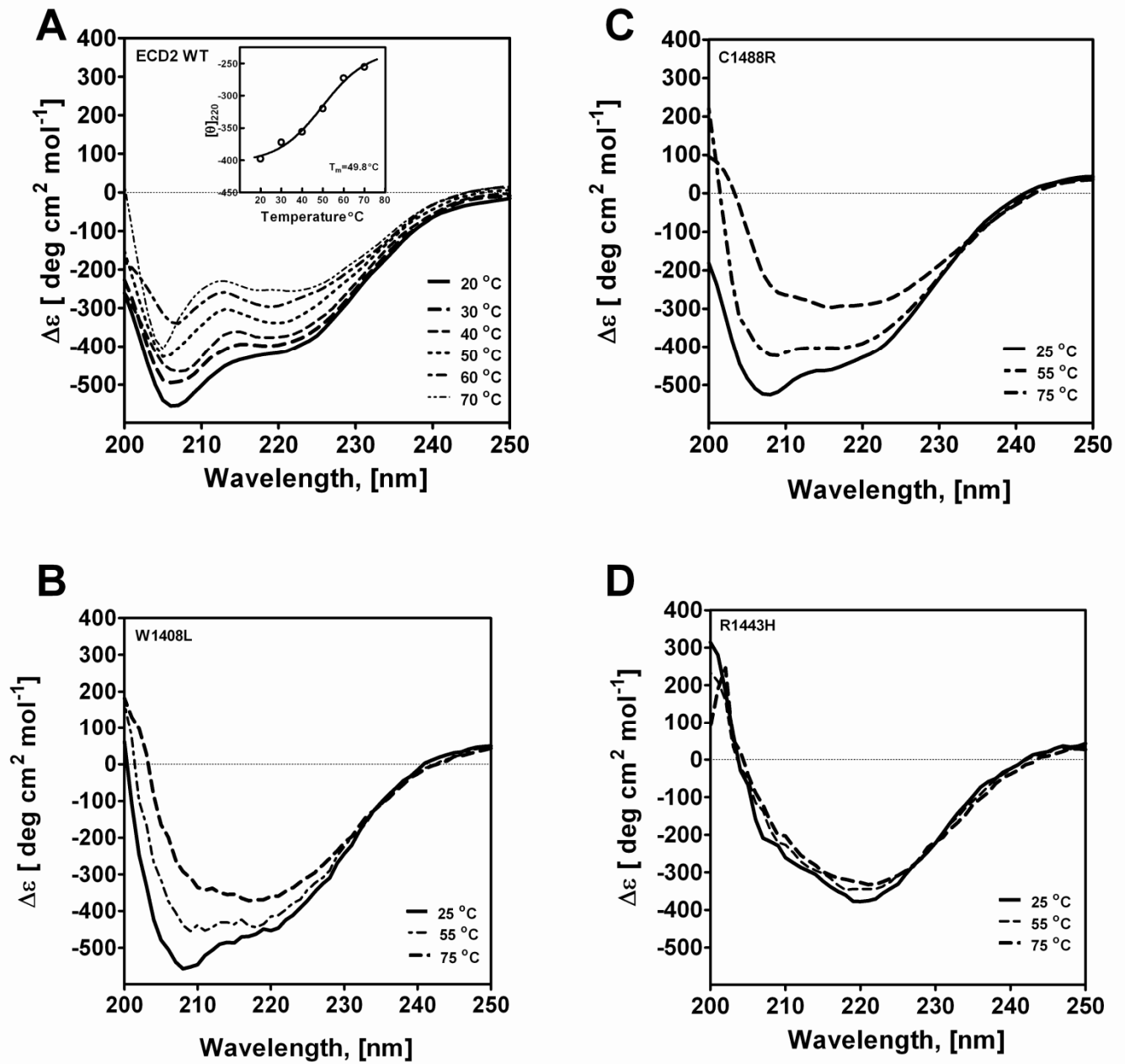


FIGURE 7

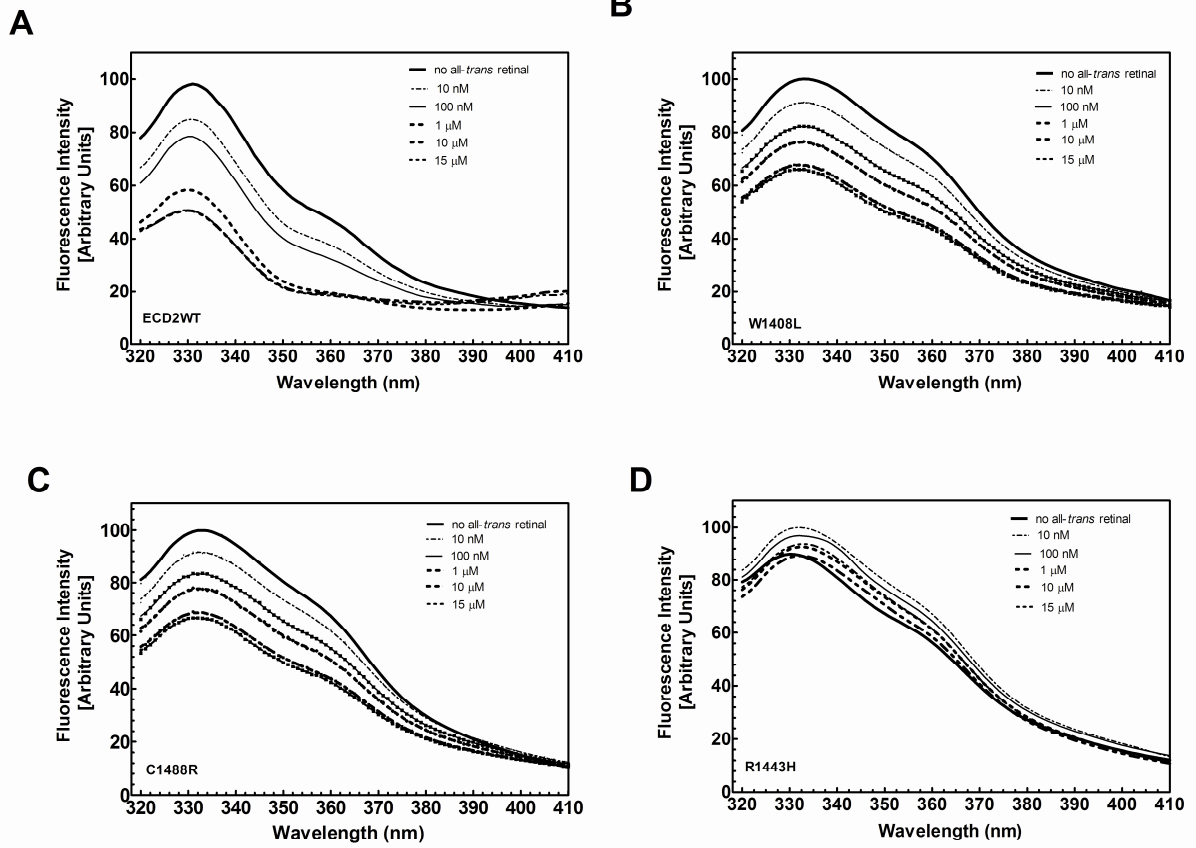


FIGURE 8

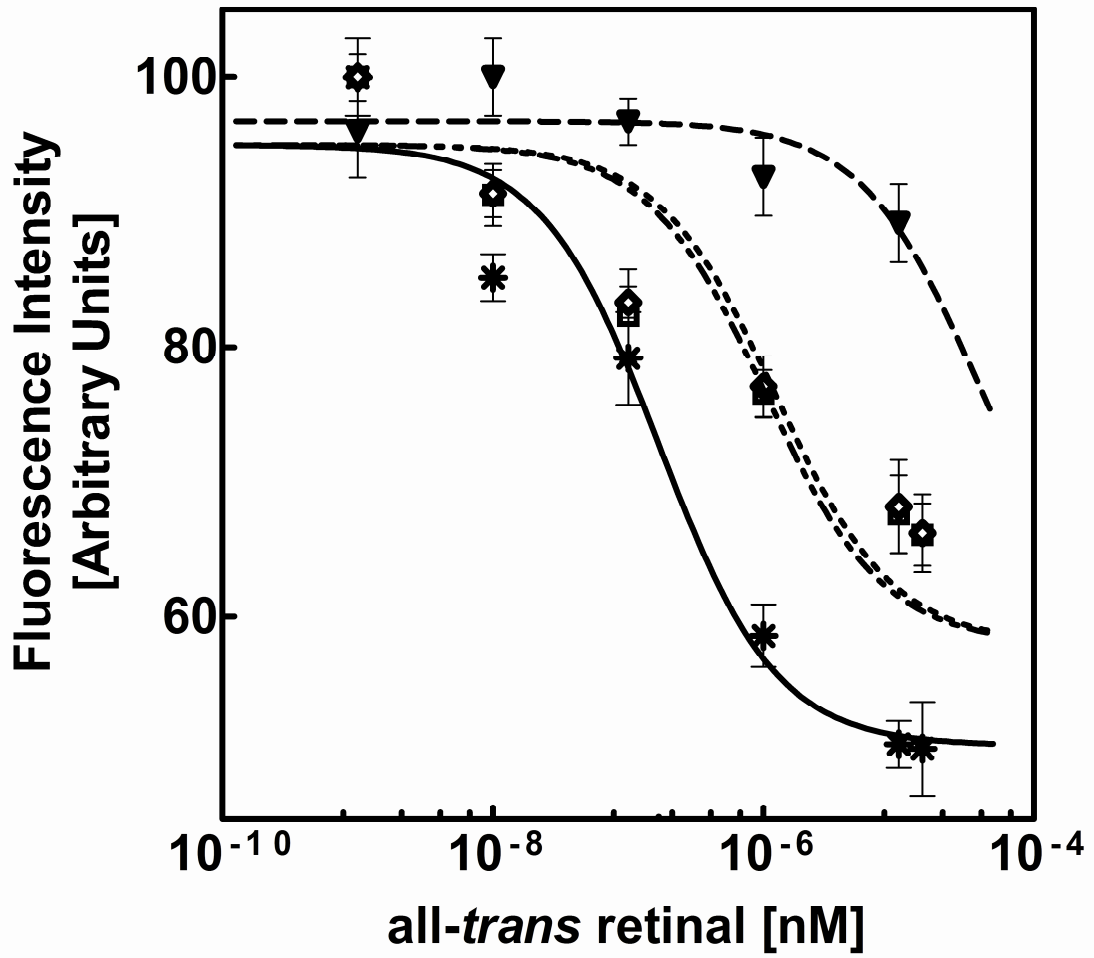


FIGURE 9

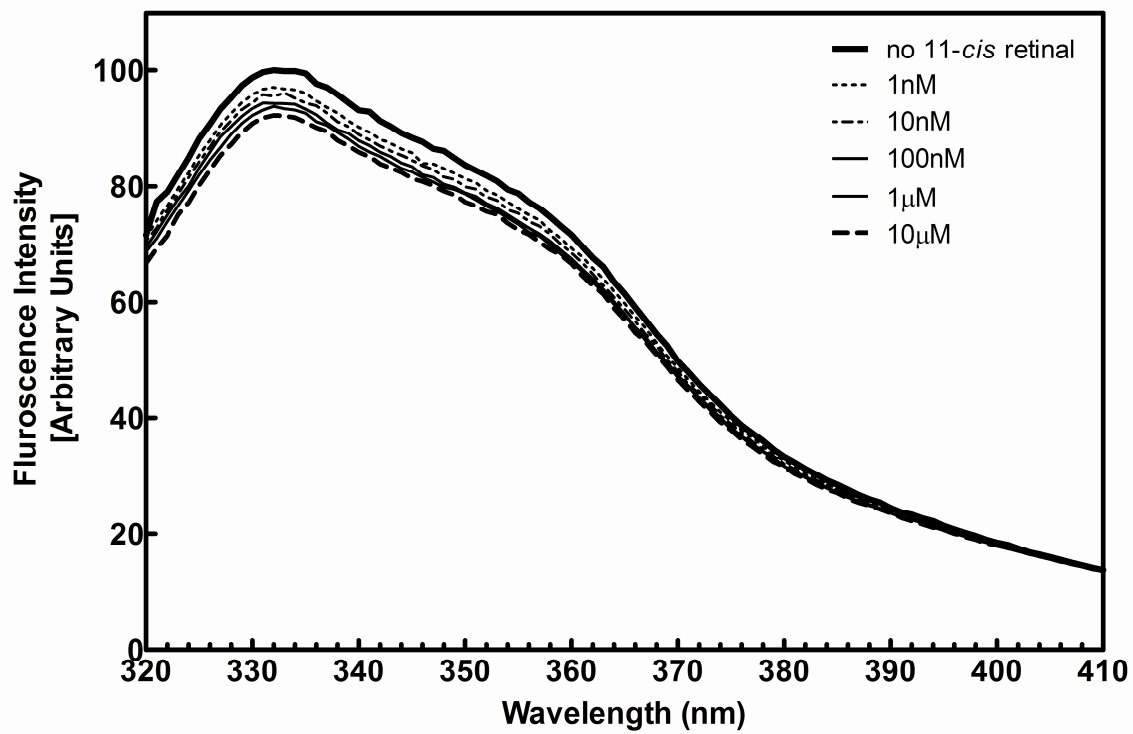


FIGURE 10

